Science of the Total Environment 646 (2019) 930–939

Contents lists available at ScienceDirect

Science of the Total Environment

journal homepage: www.elsevier.com/locate/scitotenv

Carbon emissions induced by land-use and land-cover change from 1970 to 2010 in Zhejiang, China

Enyan Zhu, Jingsong Deng *, Mengmeng Zhou, Muye Gan, Ruowei Jiang, Ke Wang, AmirReza Shahtahmassebi

College of Environmental and Resource Sciences, Zhejiang University, Hangzhou 310058, Zhejiang, China

HIGHLIGHTS

- Great changes of land-use and land-cover took place in Zhejiang during 1970 to 2010.
- Land-use and land-cover change played an important role in the carbon emissions.
- The carbon emission volume of 1990-2010 is nearly three times those of 1970-1990.
- It is essential to preserve lands with high soil organic carbon storage.

GRAPHICAL ABSTRACT

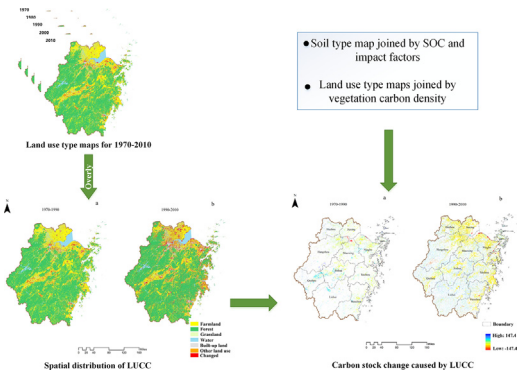
Land use type maps for 1970-2010
Overly
Soil type map joined by SOC and impact factors
Land use type maps joined by vegetation carbon density
Spatial distribution of LUCC
Carbon stock change caused by LUCC

ARTICLE INFO

Article history:
Received 19 April 2018
Received in revised form 30 June 2018
Accepted 23 July 2018
Available online 23 July 2018

Editor: R Ludwig

Keywords:
Global climate change
Carbon emission
LUCC
Vegetation carbon
SOC

ABSTRACT

Land-use and land-cover change (LUCC) is a crucial factor affecting carbon emissions. Zhejiang Province has witnessed unprecedented LUCC concomitant with rapid urbanization from 1970 to 2010. In this study, remote sensing, geographic information system (GIS) and the Intergovernmental Panel on Climate Change (IPCC) method were combined to quantify changes in both vegetation carbon storage and soil organic carbon (SOC) storage resulting from LUCC during 1970–1990 and 1990–2010. For both 1970–1990 and 1990–2010, the results showed successive decrease in farmlands (2.8×10^5 ha or −9.15% and 5.9×10^5 ha or −20.49%, respectively) and grasslands (3.4×10^4 ha or −10.73% and 1.5×10^5 ha or −54.1%, respectively), and continuous increase in forests (2.0×10^4 ha or 0.33% and 1.7×10^5 ha or 2.81%, respectively) and built-up lands (2.07×10^5 ha or 78.41% and 6.49×10^5 ha or 137.8%, respectively). From 1970 to 1990, approximately 8.3 Tg of the total carbon sink declined, including a 0.4 Tg reduction in vegetation carbon and a 7.9 Tg reduction in SOC. While from 1990 to 2010, approximately 17.5 Tg of carbon storage declined, comprising a 2.8 Tg of carbon accumulated by vegetation, and a 20.3 Tg reduction in SOC. Overall, LUCC has resulted in huge amount of carbon emissions in Zhejiang from 1970 to 2010. Efficient planning for LUCC and gradual mitigation of carbon emissions are indispensable for future urban development in China under increasing pressure from global warming.

© 2018 Published by Elsevier B.V.

1. Introduction

Global warming is an international challenge facing humanity in the 21st century (Wang et al., 2017). Since the last century, the average global surface temperature has risen by 0.74 °C (95% confidence

* Corresponding author.
E-mail addresses: eyzhu@zju.edu.cn (E. Zhu), jsong_deng@zju.edu.cn (J. Deng), mmzhou@zju.edu.cn (M. Zhou), ganmuye@zju.edu.cn (M. Gan), rwjiang@zju.edu.cn (R. Jiang), kwang@zju.edu.cn (K. Wang), amir511@zju.edu.cn (A. Shahtahmassebi).

https://doi.org/10.1016/j.scitotenv.2018.07.317
0048-9697/© 2018 Published by Elsevier B.V.

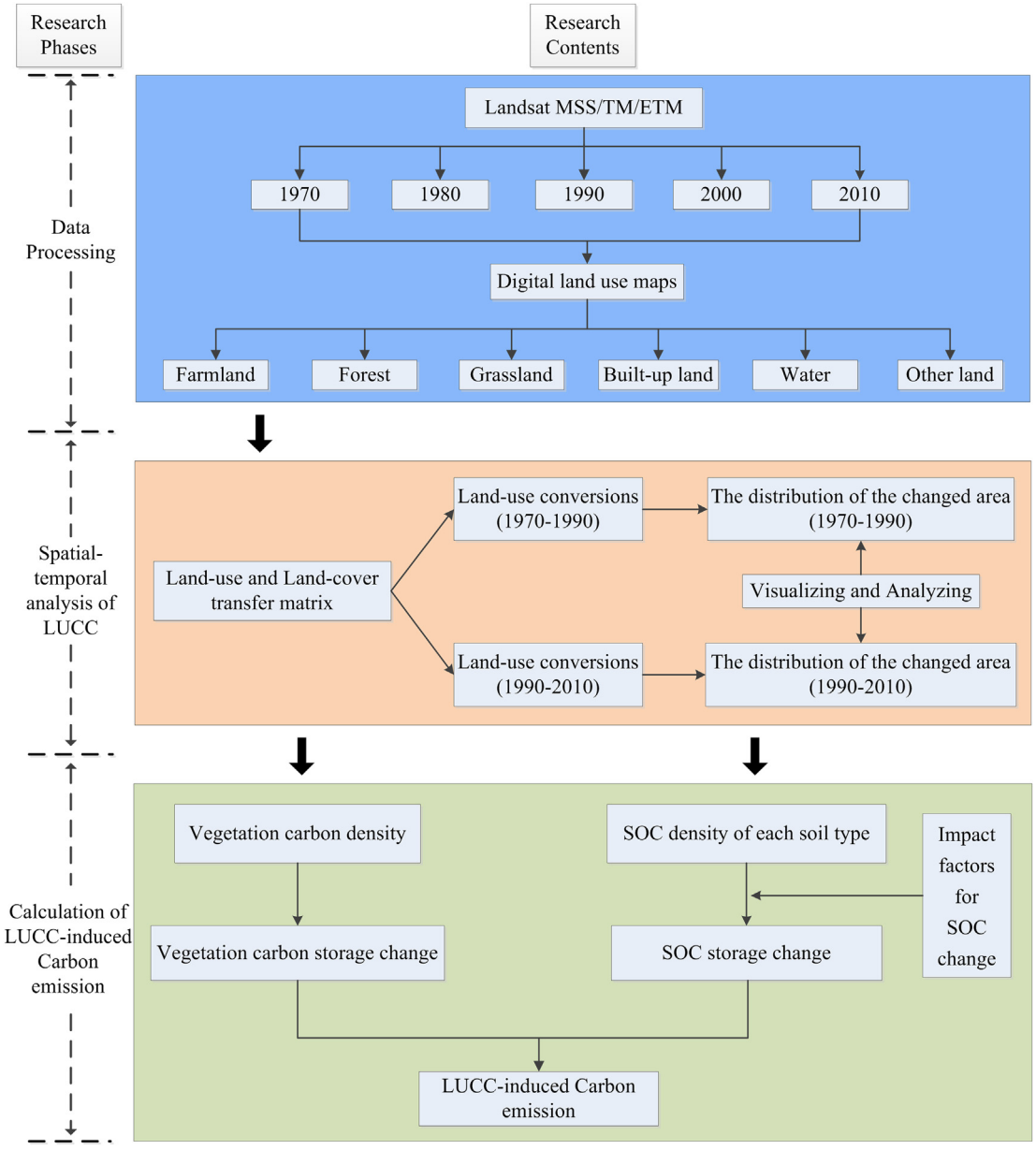

Fig. 1. Flow chart of approaches employed in this study.

interval: 0.56–0.92 °C) (Cubasch et al., 2013). At the end of 2015, 195 nations adopted the Paris Agreement under the United Nations Framework Convention on Climate Change (UNFCCC), which focused on limiting the increase in the global temperature to less than 2 °C above pre-industrial temperatures (Talks, 2015). Climate models indicate that it is still possible to achieve, but efficient and sustainable policies relating to low carbon emissions are required (Talks, 2015).

Greenhouse gas emissions (GHG), especially carbon dioxide (CO_2) emissions, are considered to be the main drivers of global warming (Bamminger et al., 2018; Cubasch et al., 2013; Yu et al., 2017). And the increase in atmospheric CO_2 concentrations has reached 1.9 ppm per year (Wang et al., 2016), which has further exacerbated global warming. Land-use and land-cover change (LUCC) is a crucial source of carbon emissions (Intergovernmental Panel on Climate Change, 2006) and accounts for approximately one-third of the carbon emissions caused by human activities since the industrial revolution (Houghton et al., 2012). Due to the significant feedback of land systems to the atmosphere, an insightful evaluation of the interaction between LUCC and carbon emission is critical.

Many studies have concentrated on the mechanisms by which land-use changes affect the carbon balance (DeFries et al., 2002; Houghton, 2002; Leite et al., 2012). These studies can be divided into two major groups: national-scale studies (Fang et al., 2007; Pilli and Grassi, 2009), and regional-scale studies (Fahey et al., 2010; Pan et al., 2003; Zhang et al., 2011). Studies of both types have focused mainly on the carbon flux of a specific ecosystem (for instance, paddies, grasslands or forests), but comparisons of the interactions between different ecosystems are lacking. Several studies have employed bookkeeping models by tracking altered areas and carbon density to calculate carbon emissions during LUCC (Dixon et al., 1994; Houghton et al., 1999; Houghton and Nassikas, 2017). The bookkeeping approach has the advantage that carbon densities and carbon response functions describing the temporal evolution and fate of carbon after a LUCC disturbance can be based directly on observational evidence (Hansis et al., 2015; Houghton et al., 2012), but has to assume that local observations can be extrapolated to regions/countries or biomes, thus partly ignoring spatial heterogeneity of carbon stocks. In several other studies, processing models have been applied to analyze the dynamic of carbon

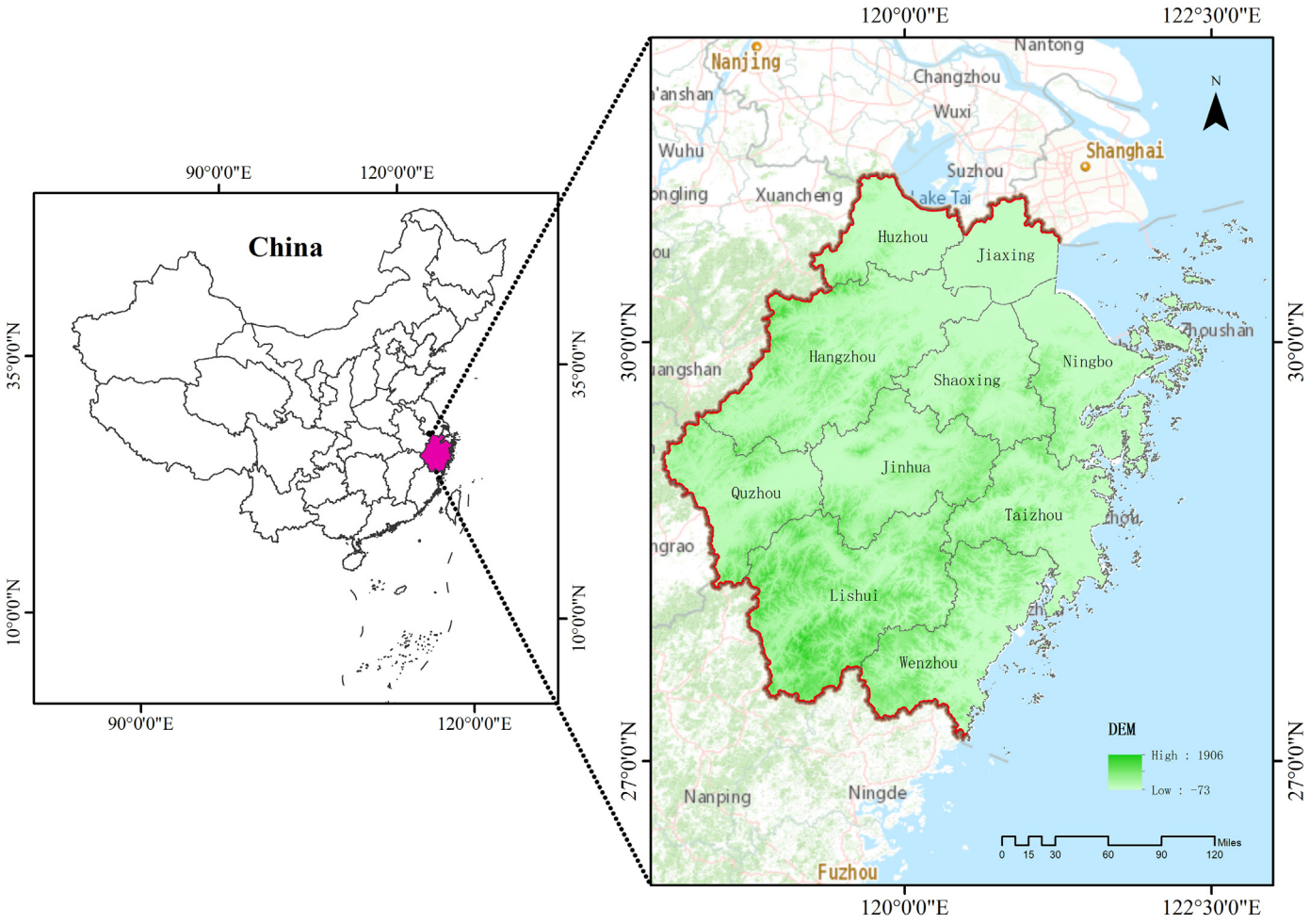

Fig. 2. Location of Zhejiang Province.

emissions during LUCC, by internally calculating carbon density of ecosystems with process-based algorithms (Han et al., 2017; Shevliakova et al., 2009). The processing-based simulations have the advantage to account for environmental effects on carbon stocks through time, but are poorly constrained by data. In addition, previous studies have been based mostly on statistics or default data sets with low precision at both the temporal and spatial scales. Hence, it would be difficult to precisely determine the spatio-temporal scales of LUCC and the corresponding induced carbon emissions.

Comprehensive analysis of the amount and spatial distribution of LUCC can provide a better understanding of its impacts on carbon emissions. More importantly, it is necessary to use data sets that provide precise information of land use and land cover. Remote sensing represents a major source of LUCC by providing spatially consistent coverage of large areas with both high spatial detail and temporal frequency, including historical time series. With increased availability and improved quality of multi-spatial and multi-temporal remote sensing data as well as new analytical techniques, it is now possible to monitor

Table 1
Land-use categories.

	Sub-categories
1 Farmland	Paddy field
	Dry farmland
2 Forest	Wood land
	Shrub land
	Sparsely forested land
	Other forested land
3 Grassland	High coverage grassland
	Middle coverage grassland
	Low coverage grassland
4 Water	River and canal
	Lake
	Reservoir and waterhole
	Tidal marsh
	Shoal and reed land
5 Built-up land	Cities and towns
	Rural settlements
	Industry and traffic land
6 Other land	Sandy land
	Gobi
	Saline-alkali land
	Swampland
	Bare land
	Rock and gravel
	Other unused land

Table 2
Vegetation carbon density for different land use types.

Land use type	Carbon density (t C ha^{-1})		
	X	X_{MIN}	X_{MAX}
Farmland	3.25	1.29	5.7
Forest	28.11	12.06	50.18
Grassland	1.24	0	2.3
Water	–	–	–
Built-up land	–	–	–
Other land	0.67	0	1.8

Note: Built-up land and water bodies were not considered for carbon accounting (Qiu et al., 2016).

Table 3
SOC density of different soil types (arranged alphabetically).

Soil type	SOC density (t C ha^{-1})	Soil type	SOC density (t C ha^{-1})
Acid sulphate soil	27.29	Gray desert soil	3.6
Alkali soil	5.33	Gray soil	94.29
Black grass felt soil	18.05	Gray forest soil	29.38
Black soil	15.42	Irrigated alluvial soil	7.21
Bleached Beijiang soils	14	Irrigated desert soil	9.52
Bog soils	49.49	Laterite	9.23
Brown coniferous forest soil	24.74	Limestone soil	13.05
Brown cool calcic soil	6.42	Meadow soil	14.43
Brown desert soil	1.15	Mountain meadow soil	26.91
Brown soil	12.81	Paddy soil	11.14
Calcic brown soil	4.25	Peaty soil	146.76
Chemozem	16.12	Purple soil	5.54
Chestnut-like calcic soil	11.06	Recent deposited soil	4.67
Chestnut-like cinnamon soil	5.61	Red clay soil	5.3
Cinnamon soil	8.25	Red soil	9.58
Cold calcic soil	6.08	Rocky soil	1.62
Cold calcic soil	6.2	Seashore solonchak soil	10.92
Cold calcic soil	3.56	Shajiang black soil	7.07
Cold calcic soil	1.21	Sierozem	5.28
Cold calcic soil	2.64	Skeleton soil	5.15
Crimson soil	9.15	Solonchak soil	6.36
Dark brown soil	18.76	Takvr soil	3.21
Desert solonchak soil	5.49	Tidal soil	6.54
Dark calcic soil	8.61	Volcanic ash soils	13.76
Dry red soil	9.2	Wind sand soil	1.91
Forest/shrub meadow soil	6.63	Yellow brown soil	13.12
Frigid solonchak soil	4.15	Yellow cinnamon soil	6.7
Grass felt soil	14.79	Yellow soft soil	3.98
Gray cinnamonic soil	13.38	Yellow soil	10.51
Gray brown desert soil	1.53		

and analyze LUCC in a timely and cost-effective way (Deng et al., 2009). In addition, being able to integrate visualization effect and geographic analysis functions with general database operations, GIS is widely used to analyze and process spatial information of LUCC (Lee, 2018; Naghibi et al., 2018). This paper aims to improve our understanding of how LUCC influence carbon emissions. Utilizing the digital land-use maps and satellite data, we firstly quantified temporal and spatial changes in land-use category conversions. Then we calculated carbon emissions induced by LUCC by matching carbon density to the actual area. Finally the spatio-temporal patterns of LUCC-induced carbon emissions from 1970 to 1990, 1990–2010 were analyzed. Zhejiang Province provides a suitable case study. As a heavily populated and rapidly developing coastal region in China, Zhejiang Province has experienced a tremendous amount of LUCC over the past few decades. However, little research has estimated the carbon emissions driven by LUCC throughout the province. In this study, we performed a spatio-temporal analysis of LUCC-induced carbon emissions in Zhejiang Province during 1970–1990 and 1990–2010, and proposed some suggestions for implementing appropriate land use policy to wisely control LUCC, and thus reducing carbon emissions.

2. Materials and methods

The overall approach employed in this study (Fig. 1) is involved refining digital land use maps for 1970, 1980, 1990, 2000 and 2010, mapping their spatial distribution and computing the changes between study periods by conducting of land-use and land-cover transfer matrix in the GIS environment. Then assign vegetation carbon density and SOC density to each land-use type. The vegetation carbon storage change was calculated by multiplying vegetation carbon density and changed areas, and the SOC storage change was calculated by multiplying SOC density and impact factors and changed areas. Finally, the total carbon storage change was calculated as the sum of vegetation carbon storage change and SOC storage change.

2.1. Study area

This study was performed in Zhejiang Province, which located along the southeastern coast of China (118°01′–123°10′E, 27°06′–31°11′N) (Fig. 2) (Yang et al., 2018). Zhejiang is a microcosm of the country's economic development as one of the most developed provinces in China (Shaohui, 2016). As a coastal province, it has experienced rapid social and economic development since the implementation of the Reform and Opening-Up Policy in 1978 (Ramankutty et al., 2002). The economic boom has sharply increased the amount of commercial, residential, and industrial built-up areas and the population, at the expense of a sharp decline in non-urban land-cover types, such as farmland, grassland and forest (Lin et al., 2017), accompanied by a surge in carbon emissions (Yang et al., 2018).

2.2. Data sets and pre-processing

The following data sets and procedures were used to carry out the study: (1) Series of Landsat images (Landsat MSS with a spatial resolution of 80 m; Landsat TM and ETM with a spatial resolution of 30 m) acquired around 1970, 1980, 1990, 2000 and 2010 were downloaded from Geospatial Data Cloud Website (http://www.gscloud.cn/) and processed. (2) Digital land-use maps for 1970, 1980, 1990, 2000 and 2010 were provided by the Chinese Ministry of Environmental Protection, with a spatial resolution of 30 m and refined by ground surveys and remote sensing interpretation (Landsat MSS/TM/ETM and Google Earth images) to an overall accuracy surpassing 90%. Details could be seen in previous studies (Li et al., 2014; Song et al., 2015). According to the National Resources and Environment Database, the original land-use types were reclassified into six major categories: farmland, forest, grassland, built-up land, water, and other land (Table 1). Because the time required reaching a new balance of soil organic carbon (SOC) after a disturbance is at least 20 years (Wang et al., 2004), we grouped the data into two periods: 1970–1990 and 1990–2010. (3) Carbon density data for each land use type (Table 2) were collected from published work (Qiu et al., 2016). (4) SOC content data for different soil types (Table 3) were obtained from China's Second National Soil Survey (Paper, 2007; Wu et al., 2003).

2.3. Spatio-temporal analysis of LUCC

With the grouped land-use data for 1970–1990 and 1990–2010, we conducted the spatio-temporal dynamics of LUCC in the GIS environment with the following steps: First, a land-use and land-cover transfer matrix was adopted to calculate the area among the different land-use conversions during 1970–1990 (Table 7), 1990–2010 (Table 8), respectively. Second, the spatial analysis tool "Overlay" in Arc-Map 10.2 was used to visualize and analyze the distribution of LUCC for both 1970–1990 and 1990–2010 (Fig. 3).

2.4. Calculation of carbon emissions induced by LUCC

The carbon emissions from land-use changes are mainly from two sources: vegetation biomass carbon storage change and SOC storage change in topsoil (0–30 cm in this research). On the one hand, LUCC can directly remove aboveground vegetation, bringing about carbon release from plant residues. On the other hand, LUCC can affect SOC storage by affecting net primary production (NPP) and the decomposition curve of underground vegetation. It can also affect SOC storage indirectly by potentially altering the biological, chemical and physical processes of the soil, thus change the soil respiration rate. Thus, the carbon emissions from LUCC were estimated as follows (Intergovernmental Panel on Climate Change, 2006):

$$\Delta C = \Delta C_{BIOMASS} + \Delta SOC_{30} \quad (1)$$

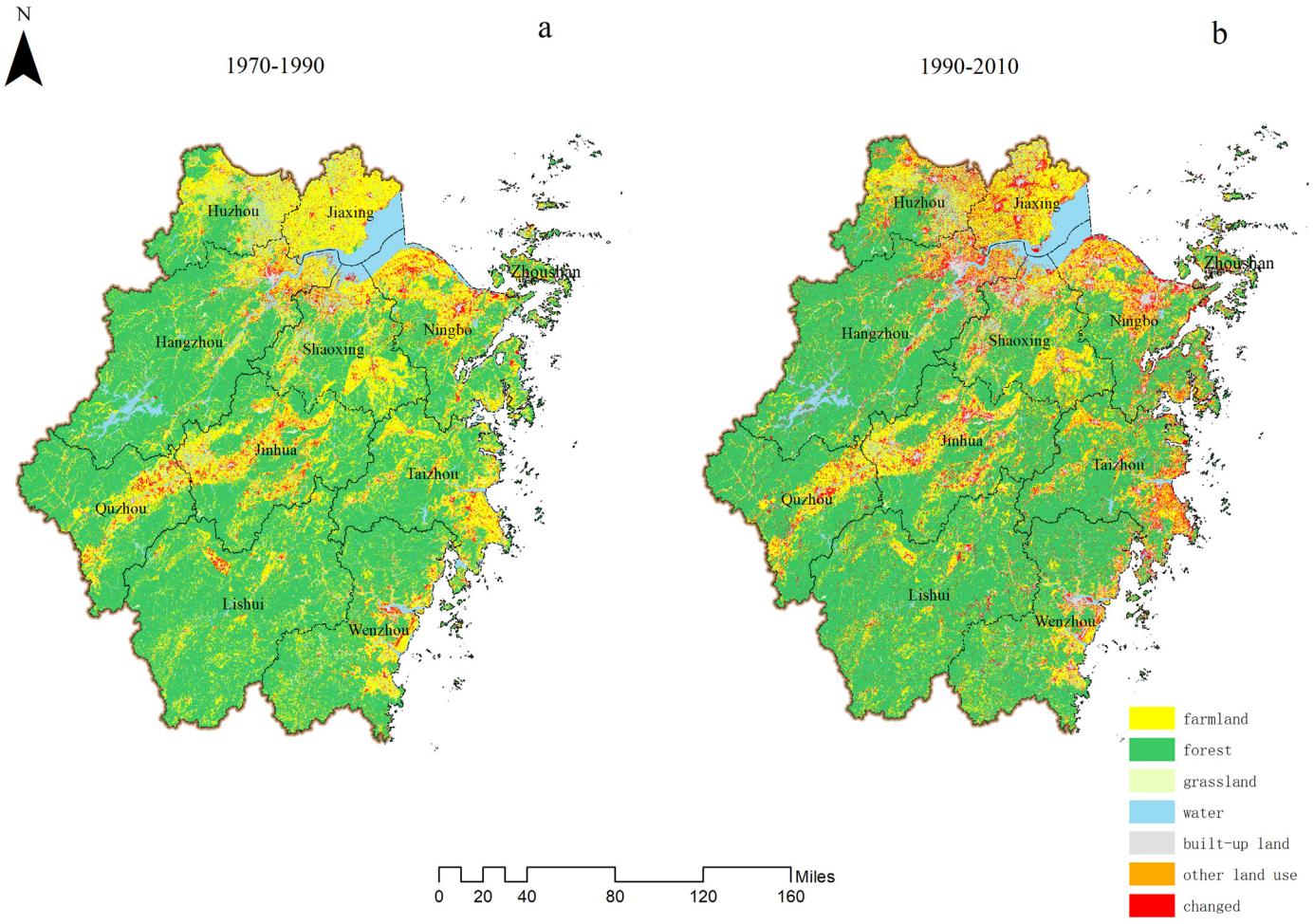

Fig. 3. Spatial distribution of LUCC in Zhejiang from 1970 to 1990 (a), 1990 to 2010 (b). The red fields represent lands transformed into a different land-use type. Others represent the lands remaining in the previous corresponding categories after transformation.

Where ΔC represents all of the carbon storage change caused by LUCC; $\Delta C_{BIOMASS}$ represents the vegetation biomass carbon storage change;ΔSOC_{30} represents the SOC storage change in the topsoil (0–30 cm).

2.4.1. Calculation of vegetation carbon storage change

Based on vegetation classification systems and the vegetation types in Zhejiang, the values of vegetation carbon density for each land use type were acquired from published results (Table 2) (Qiu et al., 2016). On the Arc-Map 10.2 platform, the digital land use maps were assigned by vegetation carbon density of each land use type. Carbon storage change of vegetation biomass caused by LUCC was calculated with the following formula (Intergovernmental Panel on Climate Change, 2006):

$$\Delta C_{vegetation} = \sum_{1}^{i}[(D_{AFTERi} - D_{BEFOREi}) \times \Delta AREAi] \quad (2)$$

Table 4
SOC impact factors for change in land-use conversion.

Items	Forest	Grassland	Farmland
Forest	–	−10%	−27%
Grassland	90%	–	−20%
Farmland	80%	100%	–

Where $\Delta C_{vegetation}$ represents the vegetation carbon storage change during LUCC; D_{AFTERi}represents the biomass carbon density on land type *i* after the conversion; $D_{BEFOREi}$ represents the biomass carbon density on land type *i* before the conversion; $\Delta AREAi$ represents the conversion area; and *i* represents the land use and land cover converted from one type to another type.

2.4.2. Calculation of SOC storage change

On the Arc-Map 10.2 platform, the 1:1 million soil type map was assigned by the SOC density (Table 3) of each soil type, which was derived from the Second National Soil Survey (Yu et al., 2005). Tier 1 method was put forward by the IPCC (Intergovernmental Panel on Climate Change, 2006) which used the soil profile statistic method to estimate the SOC storage for each patch. According to the conversion area of each land use type, and the impact factors for SOC change (Table 4) (IPCC, 2003), we applied Tier 1 method to calculate the SOC storage change caused by LUCC during 1970–1990, and 1990–2010, respectively. The SOC storage change caused by LUCC during each of these two 20-year periods was calculated using the following formula (Intergovernmental Panel on Climate Change, 2006):

$$\Delta SOC = \sum_{i,S}(SOC_{is} \times F_{IMPACTi} \times \Delta AREA_{is}) \quad (3)$$

Where ΔSOC represents the change in SOC storage; SOC_{is} represents the SOC density of land type *i* with soil type *s*; $F_{IMPACTi}$ represents the impact factors of SOC change during LUCC (Table 4) (IPCC, 2003); and

Table 5
Areas and changes in all land-use types.

Land-use type	Area in 1970	Area in 1990	Increase/decrease	Area in 2010	Increase/decrease	Increase/decrease
			Rate (1970–1990)		Rate (1990–2010)	Rate (1970–2010)
Forest	6.03×10^6	6.05×10^6	0.29%	6.22×10^6	2.78%	3.15%
Farmland	3.06×10^6	2.88×10^6	−6.03%	2.29×10^6	−20.61%	−25.16%
Grassland	3.17×10^5	2.83×10^5	−10.86%	1.30×10^5	−54.24%	−58.99%
Water	7.35×10^5	7.35×10^5	0.14%	6.87×10^5	−6.53%	−6.53%
Built-up land	2.64×10^5	4.71×10^5	78.97%	1.12×10^6	138.14%	324.24%
Other land	3.53×10^4	2.74×10^4	−23.53%	4.39×10^3	−84.62%	−87.56%

Table 6
Land use conversion matrix from 1970 to 2010 (in hectares).

1970	2010						2010 Total
	Built-up land	Farmland	Forest	Grassland	Other land	Water	
Built-up land	–	6305.34	3976.54	130.73	15.69	1531.98	11,960.29
Farmland	754,355.42	–	166,731.61	1932.53	454.81	18,693.52	942,167.89
Forest	31,045.57	3974.52	–	18.07	42.94	8791.90	43,872.99
Grassland	18,587.43	130,975.76	40,004.88	–	18.42	906.16	190,492.65
Other land	12,319.00	1217.51	17,666.96	479.44	–	317.63	32,000.54
Water	53,615.05	21,799.66	1065.63	407.75	574.26	–	77,462.36
1970 Total (ha)	869,922.47	164,272.80	229,445.63	2968.52	1106.12	30,241.19	1,297,956.73

$\Delta AREA_{is}$ represents the transformed area of land use type i with soil type s.

3. Results and discussion

3.1. Spatio-temporal dynamics of LUCC from 1970 to 2010

Zhejiang Province has witnessed enormous land-use changes during the whole period from 1970 to 2010. From the land use conversion matrix (Table 6), the area that underwent change was 1.29×10^6 ha. This represents 12.35% of the total land, at an annual rate of 0.31%. Conversions between farmland and built-up land were the major change types that occupied 72.59% of the total change. Accordingly, built-up land has altogether increased by 8.56×10^5 ha or 324.24% in area, while farmland has decreased by 7.70×10^5 ha or 25.16% in area. Other obvious changes were the declines in grassland by 1.87×10^5 ha or 58.99%. However, a net increase of 1.9×10^5 ha or 3.15% was found in forest (Table 5). Findings further indicated that farmland had the highest land changes and was the major land resources encroached by urbanization. Of the 8.56×10^5 ha increase in built-up land, 86.72% resulted from farmland conversion. Separately, the first period of 1970–1990 experienced remarkable land-use changes with 3.94×10^5 ha or 13.71% of the total area (Table 7). There was an increase of 2.07×10^5 ha in built-up land comprising 52.54% of the total land use change. Since the Reform and Opening up Policy in 1978, Zhejiang has made great efforts to attract inflows of foreign and domestic investment in the manufacturing sector. Consequently, huge tracts of land were leveled and developed into build-up land. Afterward, land reform in 1987 re-introduced land values in China, which has gradually created a property market and increased the need of housing construction. In the second period of 1990–2010, conspicuous land-use changes took place at a much larger scale than before. The conversion matrix (Table 8) shows that 34.48% (9.91×10^5 ha) of the land underwent changes with an annual growth rate of 1.72%, which was far higher than that of the previous 20 years. A total of 6.57×10^5 ha of land was converted into built-up land, accounting for approximately 66.30% of the total land changes, which almost all resulted from farmland conversion (78.87%). It is noteworthy that, due to the construction of Ecological Public Welfare Forests (EPWF), the forest area increased from 6.05×10^6 ha to 6.22×10^6 ha by 2.8%. Nevertheless, under the background of rapid economic development and urbanization, in addition to the property boom, a vast amount of lands was needed for urbanization.

With respect to the spatial pattern, spatial analysis demonstrated that for both periods, the spatial distribution tendencies of LUCC were similar (Fig. 3). The most dramatic changes took place in the northeast and coastal parts of Zhejiang, as well as in the plains in the central part, as a result of urban erosion into these regions. While in the west and southwest, where mainly occupied by rural and mountainous areas, the LUCC was slighter. Furthermore, comparing these two periods (Fig. 4) exposed significant variation in the total area of land-use conversion, for which the changed area in 1990–2010 was almost three

Table 7
Land use conversion matrix from 1970 to 1990 (in hectares).

1970	1990						1990 Total (ha)
	Built-up land	Farmland	Forest	Grassland	Other land	Water	
Built-up land	–	17,614.32	187.21	391.34	–	764.40	18,957.28
Farmland	219,387.53	–	13,013.51	31,571.75	480.71	13,090.57	277,544.06
Forest	58.61	870.59	–	–	4.40	221.80	1155.41
Grassland	195.71	66,435.39	5833.91	–	5.76	361.71	72,832.49
Other land	382.04	266.83	157.04	6477.83	–	1301.38	8585.12
Water	6361.22	7801.19	114.06	323.30	223.09	–	14,822.87
1970 Total (ha)	226,385.11	92,988.33	19,305.73	38,764.22	713.97	15,739.87	393,897.23

Table 8
Land use conversion matrix from 1990 to 2010 (in hectares).

1990	2010						2010 Total (ha)
	Built-up land	Farmland	Forest	Grassland	Other land	Water	
Built-up land	–	2366.99	1768.62	140.97	8.80	1923.15	6208.52
Farmland	517,962.91	–	153,747.73	1906.07	459.09	12,579.34	686,655.14
Forest	31,427.83	3206.17	–	17.49	42.29	9255.27	43,949.05
Grassland	47,789.03	69,064.54	38,172.88	–	23.74	1249.05	156,299.24
Other land	6688.17	681.23	16,013.98	482.89	–	255.74	24,122.02
Water	52,874.93	17,996.86	1668.15	295.95	564.83	–	73,400.71
1990 Total (ha)	656,742.87	93,315.78	211,371.35	2843.37	1098.75	25,262.54	990,634.67

times greater than that in 1990–2010, reflecting the rapid growth of urban expansion. It is consistent with the results reported in other research: from the 1990s, especially since 2000, accelerated socio-economic development has taken place in Zhejiang Province (Lin et al., 2017; Song et al., 2015, 2016).

3.2. Spatio-temporal trajectory and patterns of carbon emissions induced by LUCC

Calculations of the carbon storage change during 1970–1990 and 1990–2010 illustrated that both periods suffered decreases in the total carbon storage of 8.3 Tg and 17.4 Tg, respectively, which correspond

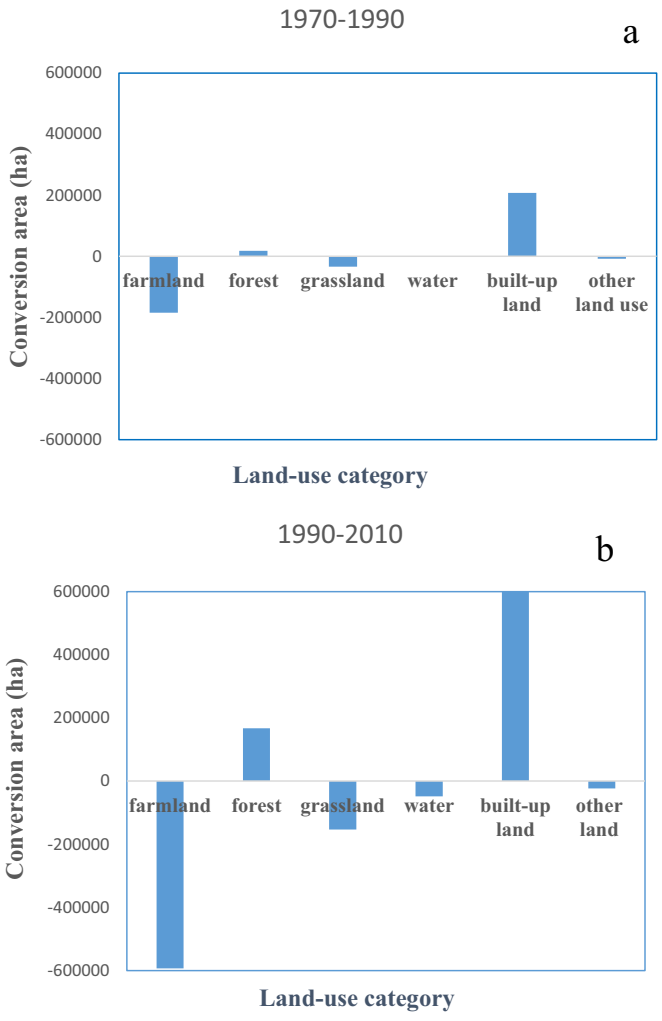

Fig. 4. Conversion areas of different land-use types from 1970 to 1990 (a) and 1990 to 2010 (b).

to decline rates of approximately 0.42 Tg year^{-1} and 0.87 Tg year^{-1}, respectively. Separately, during the first period of 1970–1990, the decline of carbon storage was 0.4 Tg in vegetation and 7.9 Tg in SOC. During the second period of 1990–2010, carbon storage in SOC decreased much more violently by 20.3 Tg, while carbon storage in vegetation increased by 2.8 Tg, offsetting more than 10% of the carbon losses of SOC. The carbon losses mainly caused by decrease of farmland with high SOC content, attributing to urban expansion. Especially during 1990–2010, when the conversion areas from the other five land-use categories (especially farmland) to built-up land occupied almost two-thirds of the total transformed area. This result was also confirmed in the spatial distribution analysis. Still worthy to mention, the increase in vegetation carbon storage during 1990 to 2010 was owing to the expansion of forest area.

With respect to the spatial pattern, for both two periods from 1790–1990 to 1990–2010, LUCC and carbon emissions were consistent in spatial distribution (Figs. 3 and 6). On the whole, with urban expansion, the northeastern plains and eastern coast were the most active regions of LUCC, where the most dramatic carbon emissions occurred. While in the west and southwest, forests increased, accordingly, carbon storages were accumulated. In addition, quantity extent and spatial distribution of carbon storage changes were also identified among the administrative districts within Zhejiang Province (Figs. 5 and 6). During the first period of 1970–1990, the maximal amount of carbon emission occurred in Taizhou city (30.16 t C/ha), followed by Shaoxing city (30.10 t C/ha), Ningbo city (29.22 t C/ha), and Jiaxing city (28.62 t C/ha). Taizhou and Ningbo are the typical coastal cities in Zhejiang which have experienced enormous land-use changes during 1970–1990, mainly reflecting in the built-up land expansion into beaches, accompanied by corresponding carbon storage loss. Dominated by plain, Shaoxing and Jiaxing are both rich in farmland resource. However, huge tracts of land were developed into build-up land and thus brought about carbon storage loss from SOC stock. Conversely, Lishui and Quzhou, two mountainous cities, have increased in carbon storage with 0.91 t C/ha and 1.32 t C/ha, respectively. Limited by topographical factors of these two regions, LUCC in these two cities was much gentler than other regions in Zhejiang Province. Additionally, the expansion of forest has also contributed to carbon accumulation in vegetation carbon storage change. During the second period of 1990–2010, the most enormous of carbon emission was also located in coastal cities and plain regions, namely Jiaxing city (126.47 t C/ha), Huzhou city (87.99 t C/ha), Taizhou city (87.88 t C/ha), and Ningbo city (71.58 t C/ha). It is apparently that with the acceleration of urban expansion, the plain city like Jiaxing and Huzhou continued to lose farmland at a faster speed, making it the most carbon-emitting region. And as a result of dramatic LUCC, coastal cities like Ningbo and Taizhou were still the most important components of carbon emission. In contrast, Lishui contributed a more pronounced increase in carbon storage with 66.42 t C/ha, owning to its substantial construction of forest reserve.

From the perspective of carbon composition, during 1970–1990, among all the administrative districts, vegetation carbon storage change was negligible, almost all of the carbon storage change were from SOC

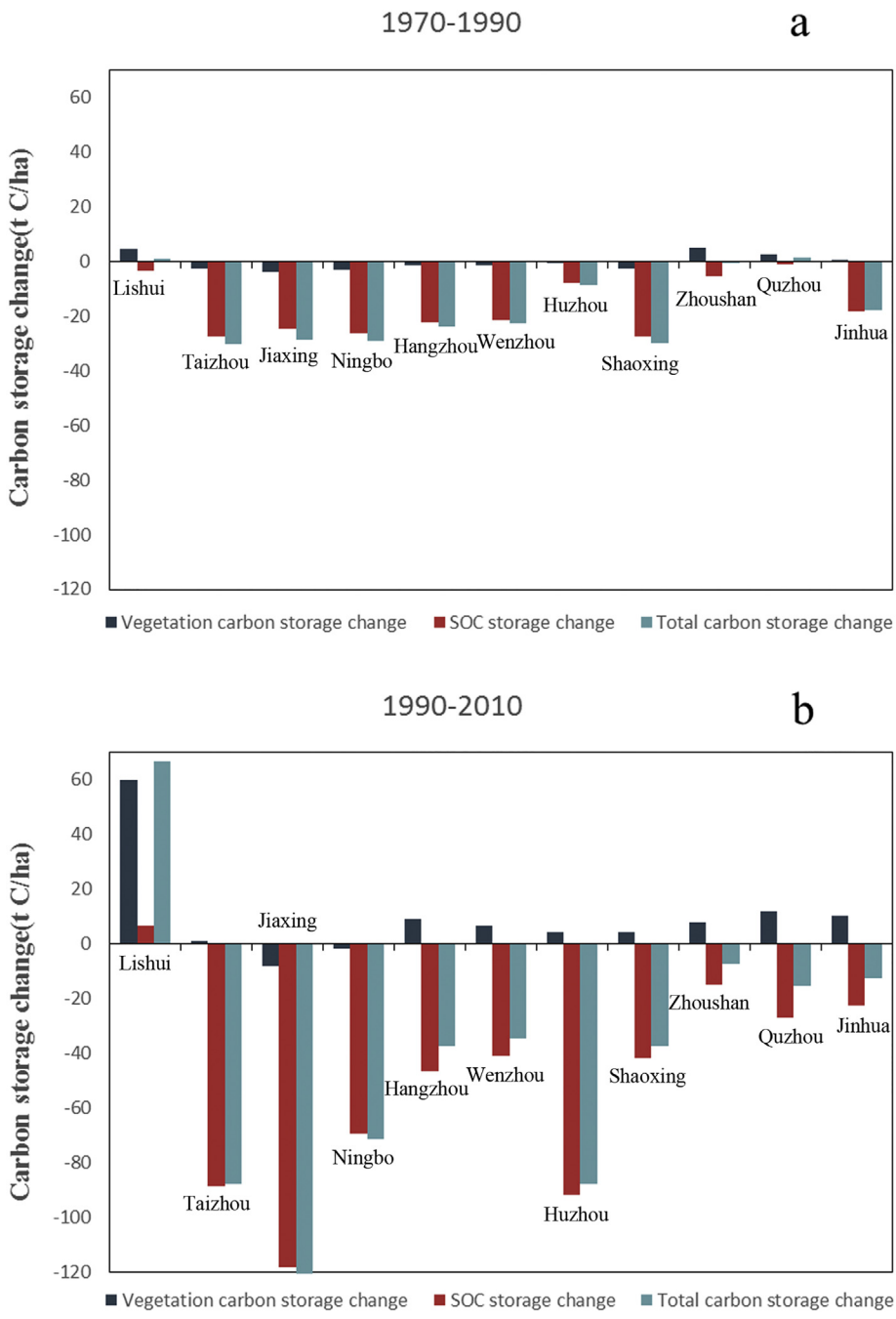

Fig. 5. Amount of carbon storage change in different administrative districts from 1970 to 1990 (a), 1990 to 2010 (b).

loss. And during 1990–2010, though most of the administrative districts accumulated carbon storage in vegetation, it was still insignificant compared to the carbon emission induced by loss of SOC. This indicated that during LUCC, the loss of underground carbon, namely, SOC, was the dominating composition of the carbon released into atmosphere.

4. Conclusion

LUCC is a global concern due to its significant influence on the carbon balance between terrestrial ecosystems and the atmosphere (Foley et al., 2005; Houghton et al., 2012). Spatio-temporal research into the LUCC-induced carbon emissions in Zhejiang Province, one of the most developed provinces in China, helps in terms of understanding policy implications in the country's other developed areas.

Between 1970 and 2010, Zhejiang's built-up land increased by almost 8.6×10^5 ha, accompanied by a loss of approximately 25 Tg of carbon from terrestrial ecosystem carbon storage. For the two periods from 1790–1990 to 1990–2010, the spatial distribution of carbon storage change presented similar patterns: Reduction in carbon storage mainly occurred in the northeast and coastal parts of Zhejiang, where the most developed cities are located. In addition, plains dominated by farming and adjoin these cities have also played a role in carbon emissions, as a result of urban expansion. While carbon accumulations were, mostly located where land has been transformed to forests, owing to ecological restoration projects such as the construction of EPWF. Through a comparison of the periods 1970–1990 and 1990–2010, we found that carbon storage loss was much more intense during the later period, which indicated

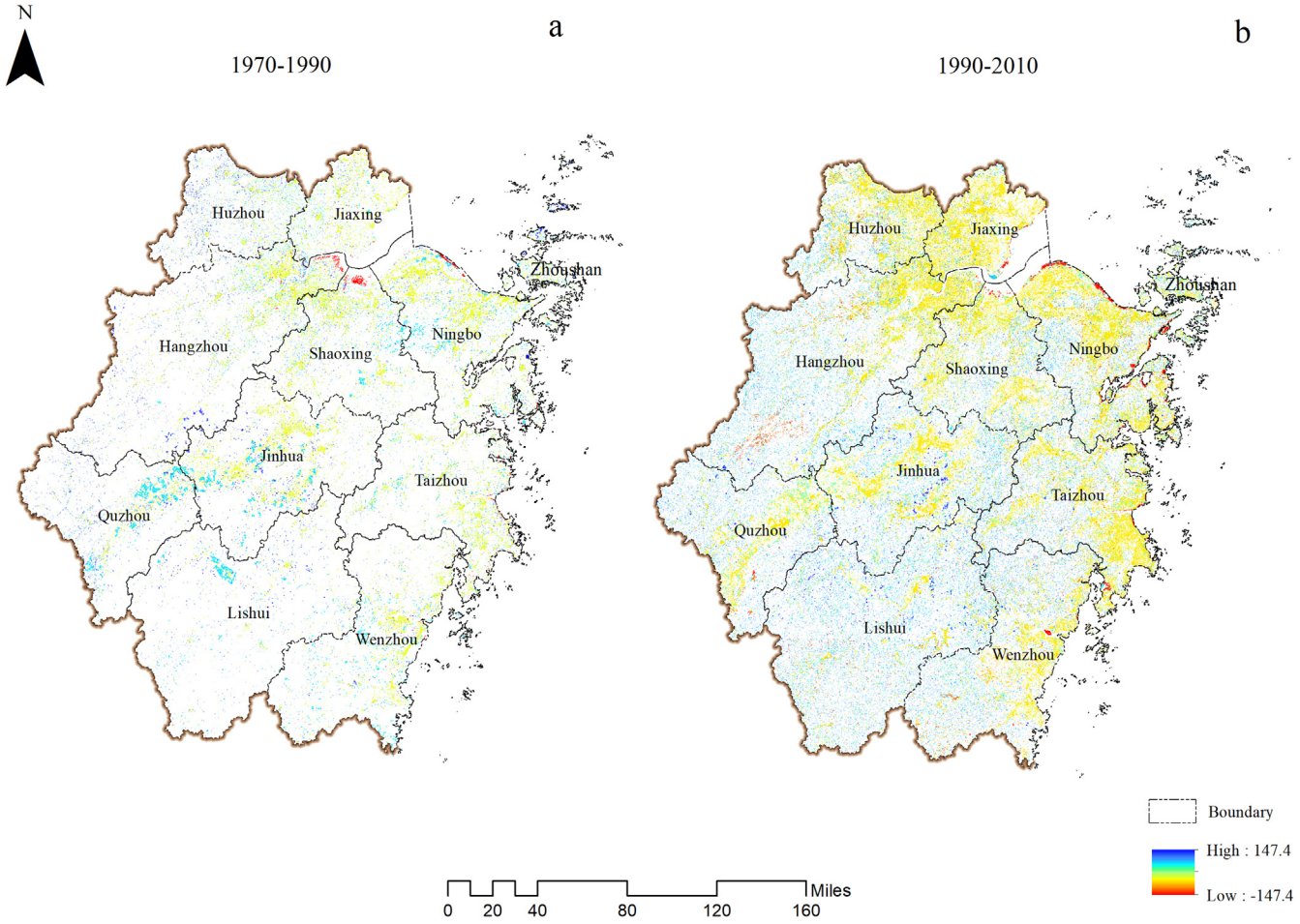

Fig. 6. Spatial distribution of carbon storage change caused by LUCC from 1970 to 1990 (a), 1990 to 2010 (b).

how rapid urbanization in Zhejiang has disturbed terrestrial ecosystem carbon balances and highlights the urgency of strengthening environmental protection. Regarding carbon composition, during LUCC over the whole period, the vegetation biomass carbon increase was approximately 0.06 Tg C year^{-1}, mainly due to the increase in forest area. Simultaneously, the SOC declined at a rate of approximately 0.71 Tg C year^{-1}, primarily due to the decline of farmland with a high SOC content, such as the Hangjiahu Plain. The results suggest that to reduce carbon emissions from LUCC, it is essential to preserve underground carbon storage by protecting lands with high SOC storage.

This study has also highlighted some important issues associated with the use of remote sensing and GIS combined method to derive information of LUCC and then estimate carbon emission, by providing spatially consistent coverage of large areas with both high spatial detail and temporal frequency. The challenge in this study was a lack of long-time ground observation data of carbon density, and this limitation may potentially lead to biases in estimation of carbon emission. For future research, long-term observation and large-scale experiment are required to collect accurate data and establish a more reliable calculation of carbon emission during LUCC.

Acknowledgments

This research was funded by the National Science-Technology Support Projects (No. 2015BAC02B06) and the Chinese Ministry of Environmental Protection Project (No. STSN-05-11).

References

Bamminger, C., Poll, C., Marhan, S., 2018. Offsetting global warming-induced elevated greenhouse gas emissions from an arable soil by biochar application. Glob. Chang. Biol. 24, e318–e334. https://doi.org/10.1111/gcb.13871.

Cubasch, U., Wuebbles, D., Chen, D., Facchini, M.C., Frame, D., Mahowald, N., Winther, J.-G., 2013. Introduction in Climate Change 2013. Intergov. Panel Clim. Chang. 2013 Phys. Sci. Basis. Contrib. Work. Gr. I to Fifth Assess. Rep. Intergov. Panel Clim. Chang. , pp. 119–158 https://doi.org/10.1017/CBO9781107415324.007.

DeFries, R.S., Houghton, R.A., Hansen, M.C., Field, C.B., Skole, D., Townshend, J., 2002. Carbon emissions from tropical deforestation and regrowth based on satellite observations for the 1980s and 1990s. Proc. Natl. Acad. Sci. 99, 14256–14261. https://doi.org/10.1073/pnas.182560099.

Deng, J.S., Wang, K., Hong, Y., Qi, J.G., 2009. Landscape and Urban Planning Spatio-temporal dynamics and evolution of land use change and landscape pattern in response to rapid urbanization. 92, 187–198. https://doi.org/10.1016/j.landurbplan.2009.05.001.

Dixon, R.K., Solomon, A.M., Brown, S., Houghton, R.A., Trexier, M.C., Wisniewski, J., 1994. Carbon pools and flux of global forest ecosystems. Science, 80 https://doi.org/10.1126/science.263.5144.185.

Fahey, T.J., Woodbury, P.B., Battles, J.J., Goodale, C.L., Hamburg, S.P., Ollinger, S.V., Woodall, C.W., 2010. Forest carbon storage: ecology, management, and policy. Front. Ecol. Environ. https://doi.org/10.1890/080169.

Fang, J.Y., Guo, Z.D., Piao, S.L., Chen, A.P., 2007. Terrestrial vegetation carbon sinks in China, 1981–2000. Sci. China Ser. D Earth Sci. 50, 1341–1350. https://doi.org/10.1007/s11430-007-0049-1.

Foley, J.A., Defries, R., Asner, G.P., Barford, C., Bonan, G., Carpenter, S.R., Chapin, F.S., Coe, M.T., Daily, G.C., Gibbs, H.K., Helkowski, J.H., Holloway, T., Howard, E.A., Kucharik, C.J., Monfreda, C., Patz, J.A., Prentice, I.C., Ramankutty, N., Snyder, P.K., 2005. Global consequences of land use. Science 309, 570–574. https://doi.org/10.1126/science.1111772.

Han, J., Meng, X., Zhou, X., Yi, B., Liu, M., Xiang, W.N., 2017. A long-term analysis of urbanization process, landscape change, and carbon sources and sinks: a case study in China's Yangtze River Delta region. J. Clean. Prod. 141, 1040–1050. https://doi.org/10.1016/j.jclepro.2016.09.177.

Hansis, E., Davis, S.J., Pongratz, J., 2015. Relevance of Methodological Choices for Accounting of Land Use Change Carbon Fluxes Special Section. https://doi.org/10.1002/2014GB004997 (Received).

Houghton, R.A., 2002. Magnitude, distribution and causes of terrestrial carbon sinks and some implications for policy. Clim. Pol. 2, 71–88. https://doi.org/10.1016/S1469-3062(02)00012-8.

Houghton, R.A., Nassikas, A.A., 2017. Global and regional fluxes of carbon from land use and land cover change 1850–2015. Glob. Biogeochem. Cycles 31, 456–472. https://doi.org/10.1002/2016GB005546.

Houghton, R.A., Hackler, J.L., Woods, T., Box, P.O., Hole, W., 1999. Emissions of carbon from forestry and land-use change in tropical Asia. Glob. Chang. Biol. 5, 481–492.

Houghton, R.A., House, J.I., Pongratz, J., Van Der Werf, G.R., Defries, R.S., Hansen, M.C., Le Quéré, C., Ramankutty, N., 2012. Carbon emissions from land use and land-cover change. Biogeosciences 9, 5125–5142. https://doi.org/10.5194/bg-9-5125-2012.

Intergovernmental Panel on Climate Change, 2006. Good Practice Guidance for Land Use, Land-Use Change and Forestry, IPCC Guidelines for National Greenhouse Gas Inventories (Prepared by the National Greenhouse Gas Inventories Programme).

IPCC, 2003. Good practice guidance for land use, land use change and forestry. Institute for Global Environmental Strategies, p. 617 (https://doi.org/citeulike-article-id:1260638).

Lee, S., 2018. Spatial Assessment of Urban Flood Susceptibility Using Data Mining and Geographic Information System (GIS) Tools [J]. Sustainability 10 (3), 648. https://doi.org/10.3390/su10030648.

Leite, C.C., Costa, M.H., Soares-Filho, B.S., De Barros Viana Hissa, L., 2012. Historical land use change and associated carbon emissions in Brazil from 1940 to 1995. Glob. Biogeochem. Cycles, 26 https://doi.org/10.1029/2011GB004133.

Li, J., Deng, J., Wang, K., Li, J., Huang, T., Lin, Y., Yu, H., 2014. Spatiotemporal patterns of urbanization in a developed region of Eastern Coastal China. Sustain. 6, 4042–4058. https://doi.org/10.3390/su6074042.

Lin, L., Ye, Z., Gan, M., Shahtahmassebi, A.R., Weston, M., Deng, J., Lu, S., Wang, K., 2017. Quality perspective on the dynamic balance of cultivated land in Wenzhou. China Sustain. 9. https://doi.org/10.3390/su9010095.

Naghibi, S.A., Pourghasemi, H.R., Abbaspour, K., 2018. A Comparison between Ten Advanced and Soft Computing Models for Groundwater Qanat Potential Assessment in Iran Using R and GIS. , pp. 967–984 https://doi.org/10.1007/s00704-016-2022-4.

Pan, G., Li, L., Wu, L., Zhang, X., 2003. Storage and sequestration potential of topsoil organic carbon in China's paddy soils. Glob. Chang. Biol. 10, 79–92. https://doi.org/10.1046/j.1529-8817.2003.00717.x.

Paper, O., 2007. Storage, patterns and environmental controls of soil organic carbon in China. , pp. 131–141 https://doi.org/10.1007/s10533-007-9109-z.

Pilli, R., Grassi, G., 2009. Bilancio del carbonio negli ecosistemi terrestri cinesi. pp. 137–139.

Qiu, L., Zhu, J., Wang, K., Hu, W., 2016. Land use changes induced county-scale carbon consequences in southeast China 1979–2020, evidence from Fuyang, Zhejiang province. Sustain. 8, 1–13. https://doi.org/10.3390/su8010038.

Ramankutty, N., Foley, J.A., Olejniczak, N.J., 2002. People on the land: changes in global population and croplands during the 20th century. Ambio 31, 251–257. https://doi.org/10.1579/0044-7447-31.3.251.

Shaohui, T., 2016. Feature: Zhejiang Export Fair serves as important bridge to boost China-Vietnam trade ties. [WWW Document]. Xinhua. http://news.xinhuanet.com/english/2016-08/05/c_135566021.htm.

Shevliakova, E., Pacala, S.W., Malyshev, S., Hurtt, G.C., Milly, P.C.D., Caspersen, J.P., Sentman, L.T., Fisk, J.P., Wirth, C., Crevoisier, C., 2009. Carbon cycling under 300 years of land use change: importance of the secondary vegetation sink. Glob. Biogeochem. Cycles 23. https://doi.org/10.1029/2007GB003176.

Song, J., Cai, D., Deng, J., Wang, K., Shen, Z., 2015. Dynamics of paddy field patterns in response to urbanization: A case study of the Hang-Jia-Hu Plain. Sustain. 7, 13813–13835. https://doi.org/10.3390/su71013813.

Song, J., Ye, J., Zhu, E., Deng, J., Wang, K., 2016. Analyzing the impact of highways associated with farmland loss under rapid urbanization. ISPRS Int. J. Geo-Information 5, 94. https://doi.org/10.3390/ijgi5060094.

Talks, P.C., 2015. The 2 °C dream. Nature 527, 436–438.

Wang, S., Huang, M., Shao, X., Mickler, R.A., Li, K., Ji, J., 2004. Vertical distribution of soil organic carbon in China. Environ. Manag. 33. https://doi.org/10.1007/s00267-003-9130-5.

Wang, G., Zhang, L., Zhuang, Q., Yu, D., Shi, X., Xing, S., Xiong, D., Liu, Y., 2016. Quantification of the soil organic carbon balance in the Tai-Lake paddy soils of China. Soil Tillage Res. 155, 95–106. https://doi.org/10.1016/j.still.2015.08.003.

Wang, F., Shackman, J., Liu, X., 2017. Carbon Emission Fl Ow in the Power Industry and Provincial CO 2 Emissions: Evidence from Cross-Provincial Secondary Energy Trading in China. , p. 159 https://doi.org/10.1016/j.jclepro.2017.05.007.

Wu, H., Guo, Z., Peng, C., 2003. Distribution and storage of soil organic carbon in China, 17 https://doi.org/10.1029/2001GB001844.

Yang, L., Xia, H., Zhang, X., Yuan, S., 2018. What matters for carbon emissions in regional sectors? A China study of extended STIRPAT model. J. Clean. Prod. 180, 595–602. https://doi.org/10.1016/j.jclepro.2018.01.116.

Yu, D., Shi, X., Sun, W., Wang, H., Liu, Q., Zhao, Y., 2005. Estimation of China soil organic carbon storage and density based on 1:1,000,000 soil database. Ying Yong Sheng Tai Xue Bao 16, 2279–2283.

Yu, P., Han, K., Li, Q., Zhou, D., 2017. Soil organic carbon fractions are affected by different land uses in an agro-pastoral transitional zone in Northeastern China. Ecol. Indic. 73, 331–337. https://doi.org/10.1016/j.ecolind.2016.10.002.

Zhang, G., Kang, Y., Han, G., Mei, H., Sakurai, K., 2011. Grassland degradation reduces the carbon sequestration capacity of the vegetation and enhances the soil carbon and nitrogen loss. Acta Agric. Scand. Sect. B Soil Plant Sci. 61, 356–364. https://doi.org/10.1080/09064710.2010.495079.